# Least-Squares Estimation of the Common Pole-Zero Filter of Acoustic Feedback Paths in Hearing Aids

Henning Schepker, *Student Member, IEEE*, and Simon Doclo, *Senior Member, IEEE*

***Abstract*—In adaptive feedback cancellation both the convergence speed and the computational complexity depend on the number of adaptive parameters used to model the acoustic feedback paths. To reduce the number of adaptive parameters, it has been proposed to model the acoustic feedback paths as the convolution of a time-invariant common pole-zero filter and time-varying all-zero filters, enabling to track fast changes. In this paper, a novel procedure to estimate the common pole-zero filter of acoustic feedback paths is presented. In contrast to previous approaches which minimize the so-called equation-error, we propose to approximate the desired output-error minimization by employing a weighted least-squares procedure motivated by the Steiglitz–McBride iteration. The estimation of the common pole-zero filter is formulated as a semidefinite programming problem, to which a constraint based on the Lyapunov theory is added in order to guarantee the stability of the estimated pole-zero filter. Experimental results using measured acoustic feedback paths from a two microphone behind-the-ear hearing aid show that the proposed optimization procedure using the Lyapunov constraint outperforms existing optimization procedures in terms of modelling accuracy and added stable gain.**

***Index Terms*—Acoustic feedback cancellation, common part modeling, hearing aids, Lyapunov stability, semidefinite programming, Steiglitz–McBride, weighted equation-error.**

## I. Introduction

In recent years the number of hearing impaired persons supplied with an open-fitting hearing aid has been steadily increasing. While in general open-fitting hearing aids largely alleviate problems related to the occlusion effect (e.g., the perception of one's own voice), they are especially prone to acoustic feedback, which is most often perceived as howling. To reduce this problem robust and fast-adapting acoustic feedback cancellation algorithms are required.

Several solutions for reducing acoustic feedback exist (see, e.g., [1]–[4]), where adaptive feedback cancellation (AFC) seems to be the most promising approach as it theoretically allows for perfect cancellation of the feedback signal. In AFC the acoustic feedback path, i.e., the impulse response (IR) between the hearing aid receiver and the hearing aid microphone, is estimated using an adaptive filter. In general, the convergence speed and the computational complexity of an adaptive filter are determined by the number of adaptive parameters [5], [6]. To reduce the number of adaptive parameters it has therefore been proposed to model the acoustic feedback path as the convolution of two filters [7]–[10]: a fixed first filter accounting for invariant or slowly varying parts of the acoustic feedback path (e.g., transducer characteristics [8] and individual ear characteristics [9]) and an adaptive filter enabling to track fast changes (e.g., caused by moving objects around the ear). In this paper we consider the problem of estimating the fixed filter from a set of acoustic feedback paths, e.g., measured on a multi-microphone hearing aid or for different positions of the hearing aid microphone(s). The fixed filter will then correspond to parts that are common in all acoustic feedback paths and is therefore called *common part* in the remainder of this paper. The second filter is assumed to correspond to parts that are variable in each acoustic feedback path and is hence called *variable part*.

Different techniques exist to estimate a common part from a set of IRs. These include techniques based on the QR-decomposition [11] or the singular value decomposition [12] and least-squares techniques [8]–[10], [13], [14]. In this paper we focus on least-squares techniques, which aim to estimate the common and the variable part by minimizing the so-called output-error. Three different filter models for the common part have previously been considered: an all-zero filter [8], an all-pole filter [13] and the general pole-zero filter [9]. Since for the common all-pole filter and the common pole-zero filter it is not straightforward to minimize the so-called output-error, it has been proposed to minimize the so-called equation-error instead [9], [13], leading to an easier optimization problem. In addition, equation-error minimization is appealing since it has been shown in [15] for single-input-single-output (SISO) systems that it yields a stable pole-zero filter. As is shown in this paper, also for the estimation of the common pole-zero filter in single-input-multiple-output (SIMO) systems the equation-error minimization yields a stable filter. Nevertheless, it is known that pole-zero filters estimated by minimizing the equation-error typically suffer from poor estimation accuracy in the vicinity of prominent spectral regions, e.g., spectral peaks [16]. To approximate the desired output-error minimization the so-called Steiglitz–McBride iteration [17] can be applied. However, in general the stability of pole-zero filters estimated by employing the Steiglitz–McBride iteration cannot be guaranteed [18], such that the location of the poles needs to be constrained.

Different constraints for the poles have been proposed in the literature, e.g., [19], [20]. A *sufficient* condition for the stability of a pole-zero filter is the strict positive realness of the frequency

Manuscript received December 22, 2015; revised March 17, 2016 and April 12, 2016; accepted April 12, 2016. Date of publication April 14, 2016; date of current version May 27, 2016. This work was supported in part by the Research Unit FOR 1732 "Individualized Hearing Acoustics" and the Cluster of Excellence 1077 "Hearing4All," funded by the German Research Foundation and project 57142981 "Individualized acoustic feedback cancellation," funded by the German Acadamic Exchange Service. The associate editor coordinating the review of this manuscript and approving it for publication was Dr. Richard Hendriks.

The authors are with the Signal Processing Group, Department of Medical Physics and Acoustics, University of Oldenburg, Oldenburg 26111, Germany (e-mail: henning.schepker@uni-oldenburg.de; simon.doclo@uni-oldenburg.de).

Digital Object Identifier 10.1109/TASLP.2016.2554288

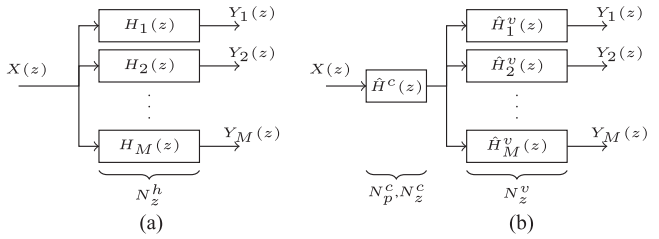


Fig. 1. System models. (a) SIMO system. (b) Approximation of SIMO system.

response of the all-pole filter component [19]. This constraint was applied to the problem of estimating the common pole-zero filter in [10]. However, since this sufficient condition may strongly restrict the solution space of the optimization problem [21], it is desirable to incorporate constraints that provide a *necessary* condition for the stability of the pole-zero filter. In [20] a constraint based on Lyapunov theory has been proposed for SISO systems, which can be formulated as a so-called linear matrix inequality (LMI) leading to a convex optimization problem [22] that can readily be solved using existing semidefinite programming (SDP) software, e.g., CVX [23], [24]. Therefore, in this paper we propose to use a constraint based on Lyapunov theory to improve the least-squares estimation of the common pole-zero filter in a SIMO system and validate the novel estimation procedure using a set of measured acoustic feedback paths.

This paper is organized as follows. In Section II the considered filter decomposition into the common pole-zero filter and the general notation are introduced. In Section III different cost functions based on the output-error criterion, the equation-error criterion and the weighted equation-error criterion are presented. In Section IV the equation-error-based optimization procedure proposed in [9] is briefly reviewed, where a two-step alternating optimization procedure is used to minimize the non-linear cost function. In Section V the Steiglitz-McBride iteration is incorporated to approximate the desired output-error minimization. Furthermore, the constraint based on the positive realness of the frequency response of the all-pole filter component is introduced and the optimization problem of estimating the common pole-zero filter is formulated as a quadratic programming (QP) problem. Finally, we propose to incorporate the Lyapunov constraint into the optimization problem and formulate the estimation of the common pole-zero filter as an SDP problem leading to a novel optimization procedure for the problem at hand. In Section VI the performance of the three optimization procedures is compared in terms of their estimation accuracy, residual output-error and added stable gain (ASG) using measured acoustic feedback paths from a two-microphone behind-the-ear hearing aid. Additionally, we compare the different common parts when used in a state-of-the-art AFC algorithm demonstrating the improved performance of the proposed SDP formulation.

## II. Scenario and Notation

Consider a SIMO system with $M$ outputs as depicted in Fig. 1(a), where the output signal $Y_m(z)$ in the $m$th microphone is related to the input signal $X(z)$ by the $m$th acoustical transfer function (ATF) $H_m(z)$, i.e.,

$$Y_m(z) = H_m(z)X(z). \tag{1}$$

Such a SIMO system arises in a single-loudspeaker multiple-microphone setup like a multi-microphone hearing aid. We assume that the true (e.g., measured) ATFs $H_m(z)$, $m = 1,\ldots,M$ can be represented by causal all-zero filters of finite order $N_z^h$, i.e.,

$$H_m(z) = \sum_{j=0}^{N_z^h} h_m[j]z^{-j}. \tag{2}$$

In order to reduce the number of parameters required to model all $M$ ATFs $H_m(z)$, the approximation as depicted in Fig. 1(b) can be used, where the estimated ATFs $\hat{H}_m(z)$ are decomposed into two parts: a microphone-independent *common part* $\hat{H}^c(z)$ and a microphone-dependent *variable part* $\hat{H}_m^v(z)$, i.e.,

$$\boxed{\begin{bmatrix} H_1(z) \\ \vdots \\ H_M(z) \end{bmatrix} \approx \begin{bmatrix} \hat{H}_1(z) \\ \vdots \\ \hat{H}_M(z) \end{bmatrix} = \hat{H}^c(z) \begin{bmatrix} \hat{H}_1^v(z) \\ \vdots \\ \hat{H}_M^v(z) \end{bmatrix}} \tag{3}$$

Assuming that $\hat{H}^c(z)$ is a pole-zero filter with $N_p^c$ poles and $N_z^c$ zeros and $\hat{H}_m^v(z)$, $m = 1,\ldots,M$ are all-zero filters with $N_z^v$ zeros each, their respective transfer functions can be written as

$$\hat{H}^c(z) = \frac{B^c(z)}{A^c(z)} = \frac{\sum_{j=0}^{N_z^c} b^c[j]z^{-j}}{1 + \sum_{j=1}^{N_p^c} a^c[j]z^{-j}}, \tag{4}$$

$$\hat{H}_m^v(z) = B_m^v(z) = \sum_{j=0}^{N_z^v} b_m^v[j]z^{-j}, \tag{5}$$

where $b^c[j]$, $a^c[j]$, and $b_m^v[j]$ denote the coefficients of the polynomials associated with the zeros of the common part, the poles of the common part and the zeros of the variable parts, respectively. Note that $A^c(z)$ is assumed to be a monic polynomial, i.e., $a^c[0] = 1$. In vector notation the coefficients of $H_m(z)$, $A^c(z)$, $B^c(z)$ and $B_m^v(z)$ can be defined as

$$\mathbf{h}_m = [\,h_m[0] \quad h_m[1] \quad \ldots \quad h_m[N_z^h]\,]^T, \tag{6}$$

$$\mathbf{a}^c = [\,a^c[1] \quad a^c[2] \quad \ldots \quad a^c[N_p^c]\,]^T, \tag{7}$$

$$\mathbf{b}^c = [\,b^c[0] \quad b^c[1] \quad \ldots \quad b^c[N_z^c]\,]^T, \tag{8}$$

$$\mathbf{b}_m^v = [\,b_m^v[0] \quad b_m^v[1] \quad \ldots \quad b_m^v[N_z^v]\,]^T, \tag{9}$$

where $[\cdot]^T$ denotes transpose operation. The concatenation of the variable part coefficient vectors $\mathbf{b}_m^v$ is defined as

$$\mathbf{b}^v = [\,(\mathbf{b}_1^v)^T \quad (\mathbf{b}_2^v)^T \quad \ldots \quad (\mathbf{b}_M^v)^T\,]^T. \tag{10}$$

## III. Least-Squares Optimization

The objective now is to compute the coefficient vectors $\mathbf{a}^c$, $\mathbf{b}^c$ and $\mathbf{b}^v$ minimizing the output-error between the true ATFs $H_m(z)$ and the estimated ATFs $\hat{H}_m(z)$ in the least-squares sense, i.e., minimizing the following least-squares cost

function

$$\bar{J}_{OE}(\mathbf{a}^c,\mathbf{b}^c,\mathbf{b}^v)=\sum_{m=1}^{M}\|\mathcal{Z}^{-1}\{\underbrace{H_m(z)-\frac{B^c(z)}{A^c(z)}B_m^v(z)}_{E_m^{OE}(z)}\}\|_2^2, \tag{11}$$

where $\mathcal{Z}^{-1}\{\cdot\}$ denotes the inverse z-transform. As can be seen from (11), the output-error $E_m^{OE}(z)$ is non-linear in $A^c(z)$, $B^c(z)$, and $B_m^v(z)$, such that the output-error cost function is difficult to minimize. To overcome this difficulty, instead often the so-called equation-error $E_m^{EE}(z)=A^c(z)E_m^{OE}(z)$ is minimized, i.e.,

$$\bar{J}_{EE}(\mathbf{a}^c,\mathbf{b}^c,\mathbf{b}^v)=\sum_{m=1}^{M}\|\mathcal{Z}^{-1}\{A^c(z)H_m(z)-B^c(z)B_m^v(z)\}\|_2^2. \tag{12}$$

Since the equation-error $E_m^{EE}(z)$ is non-linear in only $B^c(z)$ and $B_m^v(z)$, the equation-error cost function $\bar{J}_{EE}$ can be minimized, e.g., using an alternating least-squares (ALS) procedure [9] which will be reviewed in Section IV. Additionally, minimization of $\bar{J}_{EE}$ guarantees stability of $\frac{1}{A^c(z)}$. However, minimization of the equation-error in (12) essentially corresponds to multiplying the output-error $E_m^{OE}(z)$ with $A^c(z)$, i.e., the transfer function of the denominator of $\hat{H}^c(z)$. Hence, although being easier to optimize, minimization of the equation-error leads to an undesired weighting of the output-error. In fact, it has been noted in [16] for SISO systems that minimization of the equation-error may lead to poor estimation accuracy in the vicinity of prominent spectral regions of the frequency response of $H_m(z)$, e.g., spectral peaks. These spectral peaks are most often modeled by the poles, i.e., $\frac{1}{A^c(z)}$, and hence, by filtering the output-error with $A^c(z)$, i.e., the inverse pole filter, these regions are less weighted. However, since the maximum stable gain (MSG) [25] in hearing aids is typically largely determined by the output-error in regions of poor modeling accuracy, minimizing the equation-error in (12) to model acoustic feedback paths in hearing aids using a common pole-zero filter model contradicts the demand for a large MSG. To circumvent the undesired spectral weighting associated with the minimization of the equation-error in (12), the so-called Steiglitz-McBride iteration [17] can be included to approximate the desired output-error minimization in (11), where at each iteration $i$ the following cost function is minimized:

$$\bar{J}_{WEE}(\mathbf{a}_i^c,\mathbf{b}_i^c,\mathbf{b}_i^v)=\sum_{m=1}^{M}\|\mathcal{Z}^{-1}\{\underbrace{\frac{1}{A_{i-1}^c(z)}E_{m,i}^{EE}(z)}_{E_{m,i}^{WEE}(z)}\}\|_2^2, \tag{13}$$

where $E_{m,i}^{WEE}(z)$ denotes the weighted equation-error at iteration $i$. Thus at iteration $i$ the all-pole response of the estimated ATFs $\hat{H}_{m,i-1}(z)$ from the previous iteration, i.e., $\frac{1}{A_{i-1}^c(z)}$, is used to filter the equation-error $E_{m,i}^{EE}(z)$. By filtering $E_{m,i}^{EE}(z)$ with $\frac{1}{A_{i-1}^c(z)}$, the goal is to counteract the weighting of the output-error in the equation-error minimization. Hence, ideally, at convergence of the iterative procedure $\lim_{i\to\infty}(A_i^c(z)-A_{i-1}^c(z))=0$ and $\lim_{i\to\infty}E_{m,i}^{WEE}(z)=E_m^{OE}(z)$, i.e., the output-error is obtained. The weighted equation-error based optimization will be described in more detail in Section V. While approximating the desired output-error minimization, iterative minimization of $\bar{J}_{WEE}$ unfortunately does not guarantee stability of $\frac{1}{A_i^c(z)}$. This is true even for a stable $\frac{1}{A_{i-1}^c(z)}$, as has been shown for the SISO case in [18] by using a simple numerical example. Hence, in the weighted equation-error cost function in (13) the location of the poles of $\frac{1}{A_i^c(z)}$ needs to be constrained. This will be discussed in more detail in Section V-A–V-C.

## IV. Equation-Error Based Optimization

The goal of the equation-error based estimation is to compute the coefficient vectors $\mathbf{a}^c$, $\mathbf{b}^c$ and $\mathbf{b}^v$ minimizing the cost function $\bar{J}_{EE}$ in (12). This cost function can be reformulated in the time-domain as

$$\boxed{J_{EE}(\mathbf{a}^c,\mathbf{b}^c,\mathbf{b}^v)=\|\begin{bmatrix}\tilde{\mathbf{h}} & \tilde{\mathbf{H}}\end{bmatrix}\begin{bmatrix}1\\ \mathbf{a}^c\end{bmatrix}-\tilde{\mathbf{B}}^v\mathbf{b}^c\|_2^2} \tag{14}$$

where $\tilde{\mathbf{h}}$ is the $M(\tilde{N}_z^h+1)$-dimensional vector of concatenated and (possibly) zero-padded vectors of the true IRs, i.e.,

$$\tilde{\mathbf{h}}=[\,\tilde{\mathbf{h}}_1^T\quad\tilde{\mathbf{h}}_2^T\quad\dots\quad\tilde{\mathbf{h}}_M^T\,]^T, \tag{15}$$

$$\tilde{\mathbf{h}}_m=[\,\mathbf{h}_m^T\quad\mathbf{0}^T\,]^T, \tag{16}$$

where $\tilde{N}_z^h=\max\{N_z^h,N_z^c+N_z^v\}+N_p^c$ and $\mathbf{0}$ is a vector of zeros to achieve the desired length of the $(\tilde{N}_z^h+1)$-dimensional vector $\tilde{\mathbf{h}}_m$. $\tilde{\mathbf{H}}$ is the $M(\tilde{N}_z^h+1)\times N_p^c$-dimensional matrix of stacked convolution matrices of the zero-padded true IRs $\tilde{\mathbf{h}}_m$, i.e.,

$$\tilde{\mathbf{H}}=[\,\tilde{\mathbf{H}}_1^T\quad\tilde{\mathbf{H}}_2^T\quad\dots\quad\tilde{\mathbf{H}}_M^T\,]^T, \tag{17}$$

$$\tilde{\mathbf{H}}_m=\begin{bmatrix}0&\dots&\dots&0\\ h_m[0]&0&\ddots&\vdots\\ \vdots&\ddots&\ddots&0\\ h_m[N_p^c-1]&\ddots&\ddots&h_m[0]\\ \vdots&\ddots&\ddots&\vdots\\ h_m[N_z^h]&\ddots&\ddots&\vdots\\ 0&h_m[N_z^h]&\ddots&\vdots\\ \vdots&\ddots&\ddots&h_m[N_z^h]\\ \vdots&\ddots&\ddots&\vdots\\ 0&\dots&\dots&0\end{bmatrix}. \tag{18}$$

Note that for the construction of $\tilde{\mathbf{H}}_m$ in (18) the true IRs $\tilde{\mathbf{h}}_m$ are delayed by one sample. This is due to $A^c(z)$ being a monic

polynomial. Similarly, $\tilde{\mathbf{B}}^v$ is the $M(\tilde{N}_z^h+1)\times(N_z^c+1)$-dimensional matrix of concatenated convolution matrices of zero-padded coefficient vectors $\tilde{\mathbf{b}}_m^v$ of the variable zero coefficients $\mathbf{b}_m^v$, i.e.,

$$\tilde{\mathbf{B}}^v = [\,(\tilde{\mathbf{B}}_1^v)^T \quad (\tilde{\mathbf{B}}_2^v)^T \quad \dots \quad (\tilde{\mathbf{B}}_M^v)^T\,]^T, \tag{19}$$

$$\tilde{\mathbf{B}}_m^v = \begin{bmatrix} b_m^v[0] & \dots & 0 \\ \vdots & \ddots & \vdots \\ b_m^v[N_z^c-1] & \ddots & b_m^v[0] \\ \vdots & \dots & \vdots \\ b_m^v[N_z^v] & \ddots & \vdots \\ 0 & \ddots & \vdots \\ \vdots & \ddots & b_m^v[N_z^v] \\ \vdots & \ddots & \vdots \\ 0 & \dots & 0 \end{bmatrix}, \tag{20}$$

$$\tilde{\mathbf{b}}_m^v = [\,(\mathbf{b}_m^v)^T \quad \mathbf{0}^T\,]^T, \tag{21}$$

where similarly as in (16) $\mathbf{0}$ is a vector of zeros to achieve the desired length of the $(\tilde{N}_z^h+1)$-dimensional vector $\tilde{\mathbf{b}}_m^v$.

The minimization of $J_{EE}$ in (14) is non-linear in $\mathbf{b}^v$ and $\mathbf{b}^c$. To minimize (14), an ALS procedure can be applied as proposed in [9]. The objective of the ALS procedure is to separate the non-linear least-squares cost function (14) into two linear least-squares cost functions, which are minimized alternatingly until convergence is achieved. This is advantageous since closed-form solutions for the linear least-squares cost functions exist. At each iteration $i$ the aim of the ALS procedure is to minimize the following linear least-squares cost functions for the variable part coefficient vector $\mathbf{b}_i^v$ and the common part coefficient vectors $\mathbf{a}_i^c$ and $\mathbf{b}_i^c$

$$\boxed{\begin{cases} J_{EE}^v(\mathbf{b}_i^v) = \|\tilde{\mathbf{h}} + \tilde{\mathbf{H}}\mathbf{a}_{i-1}^c - \check{\mathbf{B}}_{i-1}^c\mathbf{b}_i^v\|_2^2 & \text{(22a)} \\ J_{EE}^c(\mathbf{a}_i^c,\mathbf{b}_i^c) = \|\tilde{\mathbf{h}} + \tilde{\mathbf{H}}\mathbf{a}_i^c - \tilde{\mathbf{B}}_i^v\mathbf{b}_i^c\|_2^2 & \text{(22b)} \end{cases}}$$

where $\tilde{\mathbf{B}}_i^v$ is the matrix $\tilde{\mathbf{B}}^v$ defined in (19) at iteration $i$, $\check{\mathbf{B}}_{i-1}^c$ is the $M(\tilde{N}_z^h+1)\times M(N_z^v+1)$-dimensional block-diagonal matrix of convolution matrices $\tilde{\mathbf{B}}_i^c$ of the zero-padded $(\tilde{N}_z^h+1)$-dimensional common zero coefficient vector $\tilde{\mathbf{b}}_{i-1}^c$, i.e.,

$$\check{\mathbf{B}}_{i-1}^c = \begin{bmatrix} \tilde{\mathbf{B}}_{i-1}^c & & \\ & \ddots & \\ & & \tilde{\mathbf{B}}_{i-1}^c \end{bmatrix}, \tag{23}$$

$$\tilde{\mathbf{b}}_{i-1}^c = [\,(\mathbf{b}_{i-1}^c)^T\ \mathbf{0}^T\,]^T, \tag{24}$$

TABLE I
MODULATION SCHEMES FOR COMPARISON

**input** $N_p^c$, $N_z^c$, $N_z^v$, $\mathbf{h}_m$ $m=1,\dots,M$
**initialize** $\mathbf{a}_0^c$, $\mathbf{b}_0^c$, $i=1$
**repeat**
*Normalize the common part all-zero coefficient vector to resolve scaling ambiguity*
$\mathbf{b}_{i-1}^c \leftarrow \mathbf{b}_{i-1}^c/\|\mathbf{b}_{i-1}^c\|_2$
*Estimate the variable part all-zero coefficient vector*
$\mathbf{b}_i^v \leftarrow \arg\min J_{EE}^v(\mathbf{b}_i^v)$
*Estimate the common part pole-zero coefficient vectors*
$\mathbf{a}_i^c, \mathbf{b}_i^c \leftarrow \arg\min J_{EE}^c(\mathbf{a}_i^c,\mathbf{b}_i^c)$
**until** convergence

and the $(\tilde{N}_z^h+1)\times(N_z^v+1)$-dimensional convolution matrix $\tilde{\mathbf{B}}_i^c$ is constructed similar to $\tilde{\mathbf{B}}_m^v$ in (20), i.e.,

$$\tilde{\mathbf{B}}_{i-1}^c = \begin{bmatrix} b_{i-1}^c[0] & \dots & 0 \\ \vdots & \ddots & \vdots \\ b_{i-1}^c[N_z^v-1] & \ddots & b_{i-1}^c[0] \\ \vdots & \dots & \vdots \\ b_{i-1}^c[N_z^c] & \ddots & \vdots \\ 0 & \ddots & \vdots \\ \vdots & \ddots & b_{i-1}^c[N_z^c] \\ \vdots & \ddots & \vdots \\ 0 & \dots & 0 \end{bmatrix}. \tag{25}$$

The solutions minimizing (22) are equal to

$$\begin{cases} \mathbf{b}_i^v = ((\check{\mathbf{B}}_{i-1}^c)^T\check{\mathbf{B}}_{i-1}^c)^{-1}(\check{\mathbf{B}}_{i-1}^c)^T(\tilde{\mathbf{h}} + \tilde{\mathbf{H}}\mathbf{a}_{i-1}^c), & \text{(26a)} \\ \begin{bmatrix}\mathbf{a}_i^c \\ \mathbf{b}_i^c\end{bmatrix} = \left(\mathbf{D}_i^T\mathbf{D}_i\right)^{-1}\mathbf{D}_i^T\tilde{\mathbf{h}}, & \text{(26b)} \end{cases}$$

where

$$\mathbf{D}_i = [\,-\tilde{\mathbf{H}}\ \tilde{\mathbf{B}}_i^v\,]. \tag{27}$$

Note that the minimization of (22) guarantees the stability of the estimated pole-zero filter (for a proof see Appendix VII). Due to the convolution of the common all-zero filter coefficients $\mathbf{b}_i^c$ and the variable all-zero filter coefficients $\mathbf{b}_{m,i}^v$, both filters can be identified only up to a constant scaling factor. To achieve a unique solution and to avoid numerical problems, prior to each iteration the common all-zero filter coefficients $\mathbf{b}_i^c$ are scaled to unit-norm. An overview of the ALS equation-error based optimization procedure of the common pole-zero filter is given in Table I.

Note that for the special case $N_z^c=0$, i.e., a common all-pole filter, a closed-form solution to (14) exists [13]. The cost function in (14) then simplifies to

$$J_{CAPZ}(\mathbf{a}^c,\mathbf{b}^v) = \|\tilde{\mathbf{h}} + \tilde{\mathbf{H}}\mathbf{a}^c - \mathbf{b}^v\|_2^2 \tag{28}$$

with closed-form solution

$$\begin{bmatrix}\mathbf{a}^c \\ \mathbf{b}^v\end{bmatrix} = (\mathbf{C}^T\mathbf{C})^{-1}\mathbf{C}^T\tilde{\mathbf{h}}, \tag{29}$$

$$\mathbf{C} = [\,-\tilde{\mathbf{H}}\ \mathbf{I}\,], \tag{30}$$

where $\mathbf{I}$ is the $M(\tilde{N}_z^h+1)\times M(N_z^v+1)$-dimensional block-diagonal matrix of $(\tilde{N}_z^h+1)\times(N_z^v+1)$-dimensional identity matrices. Note that when minimizing $J_{CAPZ}$ in (28) using the ALS procedure in (22), the ALS procedure will converge to the optimal solution in (29).

## V. Weighted Equation-Error Based Optimization

As mentioned in Section III, to circumvent the problem of poor estimation accuracy in the vicinity of spectral peaks, the objective of the weighted equation-error cost function in (13) is to incorporate the Steiglitz-McBride iteration [17], hence approximating the output-error minimization. This is accomplished by filtering the equation-error for each of the $M$ IRs at iteration $i$ with the all-pole filter $\frac{1}{A_{i-1}^c(q^{-1})}$ from the previous iteration, where $q^{-1}$ denotes the unit-delay operator, i.e, $q^{-1}h_m[k]=h_m[k-1]$. Therefore, at each iteration $i$ the aim is to minimize the time-domain cost function

$$J_{WEE}(\mathbf{a}_i^c,\mathbf{b}_i^c,\mathbf{b}_i^v) = \sum_{m=1}^{M}\|\frac{1}{A_{i-1}^c(q^{-1})}(\tilde{\mathbf{h}}_m+\tilde{\mathbf{H}}_m\mathbf{a}_i^c-\tilde{\mathbf{B}}_{m,i}^v\mathbf{b}_i^c)\|_2^2. \tag{31}$$

Since the cost function $J_{WEE}$ is non-linear in $\mathbf{b}_i^c$ and $\mathbf{b}_i^v$, similarly as for the equation-error cost function in (14), minimizing this non-linear cost function can be performed by using an ALS procedure, i.e., at each iteration $i$ the following two linear least-squares cost functions are minimized

$$\begin{cases} J_{WEE}^v(\mathbf{b}_i^v)=\|\tilde{\mathbf{h}}_i^p+\tilde{\mathbf{H}}_i^p\mathbf{a}_{i-1}^c-\check{\mathbf{B}}_{i-1}^{c,p}\mathbf{b}_i^v\|_2^2 & \text{(32a)}\\ J_{WEE}^c(\mathbf{a}_i^c,\mathbf{b}_i^c)=\|\tilde{\mathbf{h}}_i^p+\tilde{\mathbf{H}}_i^p\mathbf{a}_i^c-\tilde{\mathbf{B}}_i^{v,p}\mathbf{b}_i^c\|_2^2 & \text{(32b)}\end{cases}$$

where the superscript $p$ indicates filtered quantities. The vector $\tilde{\mathbf{h}}_i^p$ and the matrices $\tilde{\mathbf{H}}_i^p$, $\tilde{\mathbf{B}}_i^{v,p}$ and $\check{\mathbf{B}}_{i-1}^{c,p}$ are constructed similar as their non-filtered counterparts $\tilde{\mathbf{h}}$, $\tilde{\mathbf{H}}$, $\tilde{\mathbf{B}}^v$ and $\check{\mathbf{B}}^c$ in (15), (17), (19), and (23) using the filtered vectors $\tilde{\mathbf{h}}_{m,i}^p$, $\tilde{\mathbf{b}}_{m,i}^{v,p}$ and $\tilde{\mathbf{b}}_{i-1}^{c,p}$, where

$$\tilde{\mathbf{h}}_{m,i}^p = \frac{1}{A_{i-1}^c(q^{-1})}\tilde{\mathbf{h}}_m, \tag{33}$$

$$\tilde{\mathbf{b}}_{i-1}^{c,p} = \frac{1}{A_{i-1}^c(q^{-1})}\tilde{\mathbf{b}}_{i-1}^c, \tag{34}$$

$$\tilde{\mathbf{b}}_{m,i}^{v,p} = \frac{1}{A_{i-1}^c(q^{-1})}\tilde{\mathbf{b}}_{m,i}^v. \tag{35}$$

This filtering operation can be written, e.g., for (33) as

$$\begin{aligned}\tilde{h}_{m,i}^p[k] &= \frac{1}{A_{i-1}^c(q^{-1})}\tilde{h}_m[k]\\ &= \tilde{h}_m[k]-\sum_{j=1}^{N_p^c}a_{i-1}^c[j]\tilde{h}_{m,i}^p[k-j],\end{aligned} \tag{36}$$

for $k=0,\ldots,\tilde{N}_z^h$ and $\tilde{h}_{m,i}^p[k]=0$ for $k<0$. The linear least-squares problems in (32) then have similar closed-form solutions as in (26) but based on the filtered quantities, i.e.,

$$\begin{cases}\mathbf{b}_i^v=((\check{\mathbf{B}}_{i-1}^{c,p})^T\check{\mathbf{B}}_{i-1}^{c,p})^{-1}(\check{\mathbf{B}}_{i-1}^{c,p})^T(\tilde{\mathbf{h}}_i^p+\tilde{\mathbf{H}}_i^p\mathbf{a}_{i-1}^c), & \text{(37a)}\\ \begin{bmatrix}\mathbf{a}_i^c\\ \mathbf{b}_i^c\end{bmatrix}=\left((\mathbf{D}_i^p)^T\mathbf{D}_i^p\right)^{-1}(\mathbf{D}_i^p)^T,\tilde{\mathbf{h}}_i^p, & \text{(37b)}\end{cases}$$

where

$$\mathbf{D}_i^p=[\,-\tilde{\mathbf{H}}_i^p\ \tilde{\mathbf{B}}_i^{v,p}\,]. \tag{38}$$

Similarly to the alternating minimization of the equation-error in (22), the filter coefficient vectors $\mathbf{b}_i^v$ and $\mathbf{b}_i^c$ can be identified only up to a constant scalar. Therefore, prior to each iteration $\mathbf{b}_i^c$ is normalized to unit-norm.

Note that in general the common pole-zero filter estimated using (32b) is not guaranteed to be stable such that the location of the poles needs to be constrained. In the following subsections two different constraints are proposed to guarantee the stability, leading to different optimization problems. In Section V-A a sufficient but not necessary constraint based on the positive realness of the frequency response of the all-pole filter [19] is considered leading to a QP problem. In Section V-B a sufficient and necessary LMI constraint based on Lyapunov theory [20] is introduced to guarantee stability. To allow for the incorporation of LMI constraints, the optimization problem in (32b) is reformulated as an SDP in Section V-C leading to a novel optimization procedure for estimating the common pole-zero filter.

### A. Frequency-Domain Stability Constraint

Stability of a causal system is guaranteed when its poles, i.e., the roots of $A_i^c(z)$, are located strictly inside the unit circle. Since this is not guaranteed by the Steiglitz-McBride iteration employed in (32b), the location of the poles needs to be constrained. In [19] it was shown that a sufficient (but not necessary) condition for the stability of $\frac{1}{A_i^c(z)}$ is that the real part of the frequency response $A_i^c(e^{j\Omega})$ is strictly positive for all normalized frequencies $\Omega$, i.e.,

$$\mathfrak{Re}\{A_i^c(e^{j\Omega})\}>0 \quad \forall\Omega, \tag{39}$$

where $\mathfrak{Re}\{\cdot\}$ denotes the real part. To control the stability margin, a small positive constant $\delta$ is typically introduced, i.e.,

$$\mathfrak{Re}\{A_i^c(e^{j\Omega})\}\geq\delta \quad \forall\Omega. \tag{40}$$

Since (40) requires the evaluation of $A_i^c(e^{j\Omega})$ over a continuous frequency range and is hence not realizable in practice, (40) is evaluated over a dense grid of $Q+1$ discrete frequency points, i.e.,

$$\mathfrak{Re}\{\mathbf{F}\}\begin{bmatrix}1\\ \mathbf{a}_i^c\end{bmatrix}\geq\delta\mathbf{1}, \tag{41}$$

where $\mathbf{F}$ is the $(Q+1)\times(N_p^c+1)$-dimensional discrete Fourier transformation matrix and $\mathbf{1}$ is a $(Q+1)$-dimensional vector of ones. Minimizing (32b) subject to the stability

constraint in (41) corresponds to a QP problem, i.e.,

$$\min_{\mathbf{a}_i^c, \mathbf{b}_i^c} (\mathbf{e}_i^{c,p})^T \mathbf{e}_i^{c,p} \tag{42a}$$

$$\text{subject to} \quad -\mathfrak{Re}\{\mathbf{F}\} \begin{bmatrix} 1 \\ \mathbf{a}_i^c \end{bmatrix} \leq -\delta \mathbf{o} \tag{42b}$$

where

$$\mathbf{e}_i^{c,p} = \tilde{\mathbf{h}}_i^p + \tilde{\mathbf{H}}_i^p \mathbf{a}_i^c - \tilde{\mathbf{B}}_i^{v,p} \mathbf{b}_i^c \tag{43}$$

is the weighted equation-error in (32b). The QP in (42) can then be efficiently solved using, e.g., the MATLAB function `quadprog`.

### B. LMI Stability Constraint

The constraint in (41) provides a sufficient (but not necessary) condition for the stability of the common pole-zero filter may hence restrict the solution space. Furthermore, (41) requires the computation of the frequency response $A_i^c(e^{j\Omega})$ over a dense grid of $Q+1$ frequencies, requiring a careful choice of $Q$. In the following we propose to use a constraint based on Lyapunov theory [6], [20], [21] that provides a necessary and sufficient condition for the stability of the common pole-zero filter and does not require the computation of the frequency response.

Requiring the roots of $A_i^c(z)$ to be strictly located inside the unit circle is equivalent to requiring the absolute value of all eigenvalues of the canonical matrix

$$\mathbf{A}_i^c = \begin{bmatrix} -a_i^c[1] & -a_i^c[2] & \dots & -a_i^c[N_p^c] \\ 1 & & & 0 \\ & \ddots & & \vdots \\ & & 1 & 0 \end{bmatrix} \tag{44}$$

to be strictly smaller then 1. From Lyapunov theory [6] it is known that the matrix $\mathbf{A}_i^c$ corresponds to a stable IIR filter, if and only if there exists a positive definite matrix $\mathbf{P}_i$, such that the following relation holds

$$\mathbf{P}_i - (\mathbf{A}_i^c)^T \mathbf{P}_i \mathbf{A}_i^c \succ \emptyset, \tag{45}$$

where $\succ \emptyset$ denotes positive definiteness. Although (45) is a necessary condition for stability, it is important to realize that it cannot be implemented directly as an LMI constraint, since it requires the joint estimation of $\mathbf{P}_i$ and $\mathbf{A}_i^c$. Therefore, at each iteration $i$ the positive definite matrix $\tilde{\mathbf{P}}_i$ is first computed by solving the Lyapunov equation using the matrix $\mathbf{A}_{i-1}^c$ from the previous iteration, i.e.,

$$\tilde{\mathbf{P}}_i - (\mathbf{A}_{i-1}^c)^T \tilde{\mathbf{P}}_i \mathbf{A}_{i-1}^c = \mathbf{I} \quad s.t.\ \tilde{\mathbf{P}}_i \succ \emptyset. \tag{46}$$

Using $\tilde{\mathbf{P}}_i$ computed from (46), the constraint in (45) is then reformulated by requiring

$$\tilde{\mathbf{P}}_i - (\mathbf{A}_i^c)^T \tilde{\mathbf{P}}_i \mathbf{A}_i^c - \tau \mathbf{I} \succeq \emptyset, \tag{47}$$

where $\tau$ is a small positive constant to control the stability margin and $\succeq \emptyset$ denotes positive semi-definiteness. Note that since $\mathbf{A}_i^c$ now appears affinely in (47) it can be formulated as an LMI by recognizing the Schur complement [22] in (47), i.e.,

$$\boldsymbol{\Gamma}_i^{stab} = \begin{bmatrix} \tilde{\mathbf{P}}_i - \tau \mathbf{I} & (\mathbf{A}_i^c)^T \\ \mathbf{A}_i^c & \tilde{\mathbf{P}}_i^{-1} - \tau \mathbf{I} \end{bmatrix} \succeq \emptyset. \tag{48}$$

Note that the constraint in (48) is no longer a necessary but a sufficient condition for stability since $\tilde{\mathbf{P}}_i$ has been computed from the previous $\mathbf{A}_{i-1}^c$. Nevertheless, it has been noted in [26] for the design of SISO pole-zero filters that the constraint will become less strict as the iterative procedure converges, i.e., $\lim_{i\to\infty}(\mathbf{A}_i^c - \mathbf{A}_{i-1}^c) = \mathbf{0}$.

### C. SDP Formulation of (32b)

To be able to use the constraint in (48) guaranteeing stability of the common pole-zero filter, the minimization in (32b) is also reformulated as an LMI, which can then be solved using SDP [22]. To write $J_{WEE}^c$ in (32b) as an LMI first the so-called auxiliary variable $t$ is introduced which provides an upper bound on the cost, i.e., the minimization in (32b) can be reformulated as

$$\min_{\mathbf{a}_i^c, \mathbf{b}_i^c} \quad t \tag{49a}$$

$$\text{subject to} \quad (\mathbf{e}_i^{c,p})^T \mathbf{e}_i^{c,p} \leq t \tag{49b}$$

Rewriting (49b) as $t - (\mathbf{e}_i^{c,p})^T \mathbf{e}_i^{c,p} \geq 0$ and recognizing the Schur complement minimizing (49) subject to the constraint (48) can be written as an SDP, i.e.,

$$\min_{\mathbf{a}_i^c, \mathbf{b}_i^c} \quad t \tag{50a}$$

$$\text{subject to} \quad \begin{bmatrix} t & (\mathbf{e}_i^{c,p})^T \\ \mathbf{e}_i^{c,p} & \mathbf{I} \end{bmatrix} \succeq \emptyset \tag{50b}$$

$$\boldsymbol{\Gamma}_i^{stab} \succeq \emptyset \tag{50c}$$

where $\mathbf{I}$ is the $M(\tilde{N}_z^h + 1) \times M(\tilde{N}_z^h + 1)$-dimensional identity matrix. The SDP in (50) can be efficiently solved using interior-point methods [22], e.g., implemented in the convex optimization toolbox CVX [23], [24]. An overview of the proposed weighted equation-error based optimization procedure of the common pole-zero filter optimizing either the QP problem in (42) or the novel SDP problem in (50) is given in Table II.

## VI. Experimental Evaluation

In this section the optimization procedures minimizing the equation-error (cf., Table I) and the weighted equation-error (cf., Table II) are experimentally compared using measured acoustic feedback paths. In Section VI-A the used acoustic setup and the considered performance measures are introduced. In Section VI-B the effect of different initializations on the performance is investigated. In Section VI-C the resulting amplitude responses of the output-error are compared and the improved accuracy of the proposed weighted equation-error optimization procedure using a stability constraint based on Lyapunov theory is demonstrated in Section VI-D. In Section VI-E the performance is investigated for unknown acoustic feedback paths that were not included in the optimization of the common pole-zero filter. In Section VI-F simulations are performed comparing the

TABLE II
OVERVIEW OF THE OPTIMIZATION PROCEDURES TO MINIMIZE THE WEIGHTED EQUATION-ERROR (31)

**input** $N_p^c$, $N_z^c$, $N_z^v$, $\mathbf{h}_m$ $m = 1, \ldots, M$
**initialize** $\mathbf{a}_0^c$, $\mathbf{b}_0^c$, $i = 1$
**repeat**
  *Normalize the common part all-zero coefficient vector to resolve scaling ambiguity*
  $\mathbf{b}_{i-1}^c \leftarrow \mathbf{b}_{i-1}^c / \|\mathbf{b}_{i-1}^c\|_2$
  *Filter the IRs and the common all-zero coefficient vector*
  $\tilde{\mathbf{h}}_{m,i}^p \leftarrow (A_{i-1}^c(q))^{-1}\tilde{\mathbf{h}}_m$, $m = 1, \ldots, M$
  $\tilde{\mathbf{b}}_{i-1}^{c,p} \leftarrow (A_{i-1}^c(q))^{-1}\tilde{\mathbf{b}}_{i-1}^c$
  *Estimate the variable part all-zero coefficient vector*
  $\mathbf{b}_i^v \leftarrow \arg\min J_{WEE}^v(\mathbf{b}_i^v)$, cf. (32a)
  *Filter the variable part all-zero coefficient vector*
  $\tilde{\mathbf{b}}_{m,i}^{v,p} = (A_{i-1}^c(q))^{-1}\tilde{\mathbf{b}}_{m,i}^v$
  **if** QP **then**
    *Estimate the common part pole-zero coefficient vectors*
    $\mathbf{a}_i^c, \mathbf{b}_i^c \leftarrow$ solve the QP in (42)
  **else if** SDP **then**
    *Solve the Lyapunov equation*
    $\tilde{\mathbf{P}}_i \leftarrow$ solve $\tilde{\mathbf{P}}_i - (\mathbf{A}_{i-1}^c)^T\tilde{\mathbf{P}}_i\mathbf{A}_{i-1}^c = \mathbf{I} \quad s.t.\ \tilde{\mathbf{P}}_i \succ \mathbf{0}$
    *Estimate the common part pole-zero coefficient vectors*
    $\mathbf{a}_i^c, \mathbf{b}_i^c \leftarrow$ solve the SDP in (50) s.t. $\mathbf{\Gamma}_i^{stab}$ in (48)
  **end if**
**until** convergence

common pole-zero filter obtained from the different optimization procedures when the common part decomposition is applied in a state-of-the-art AFC algorithm.

### A. Acoustic Setup, Performance Measures and Algorithm Parameters

Acoustic feedback paths were measured using a two-microphone behind-the-ear hearing aid with open-fitting earmolds. To account for differences in acoustic feedback paths, e.g., due to different ear canal geometries a dummy head with adjustable ear canals similar to [27] was used. In total $M = 8$ acoustic feedback paths were measured, i.e., using two microphones for two different acoustic scenarios and for two different ear canals, hence simulating variability across acoustics and subjects. The first set of four IRs, $m = 1, 2, 3, 4$ was measured using an ear canal diameter of $d_1 = 7$ mm and a length of $l_1 = 15$ mm, while the second set of four IRs, $m = 5, 6, 7, 8$ was measured using $d_2 = 8$ mm and $l_2 = 20$ mm. The IRs $m = 1, 2, 5, 6$, were measured in free field, i.e., no obstruction was in close distance to the dummy head, while IRs $m = 3, 4, 7, 8$ were measured with a telephone receiver positioned in close distance to the dummy heads ear. An overview of all acoustic feedback paths used in the experimental evaluation is given in Table III. All IRs were sampled using a sampling frequency of $f_s = 16\,000$ Hz and truncated to order $N_z^h = 99$.

Figs. 2 and 3 depict the amplitude and phase responses of the IRs for the first ear canal setting ($d_1 = 7$ mm and $l_1 = 15$ mm) and for the second ear canal setting ($d_2 = 8$ mm and $l_2 = 15$ mm), respectively. In general, for each set all four IRs share a great similarity, which could possibly be exploited by means of a common pole-zero filter. Only the fourth IR in the first ear canal setting differs substantially from the other three IRs in the frequency regions between 5500 Hz and 6500 Hz due to the presence of the telephone receiver.

TABLE III
OVERVIEW OF THE ACOUSTIC FEEDBACK PATHS USED IN THE EXPERIMENTAL EVALUATION

| $m$ | $d$ | $l$ | Acoustic condition |
|---|---|---|---|
| 1 | 7 mm | 15 mm | free field |
| 2 | 7 mm | 15 mm | free field |
| 3 | 7 mm | 15 mm | telephone |
| 4 | 7 mm | 15 mm | telephone |
| 5 | 8 mm | 20 mm | free field |
| 6 | 8 mm | 20 mm | free field |
| 7 | 8 mm | 20 mm | telephone |
| 8 | 8 mm | 20 mm | telephone |

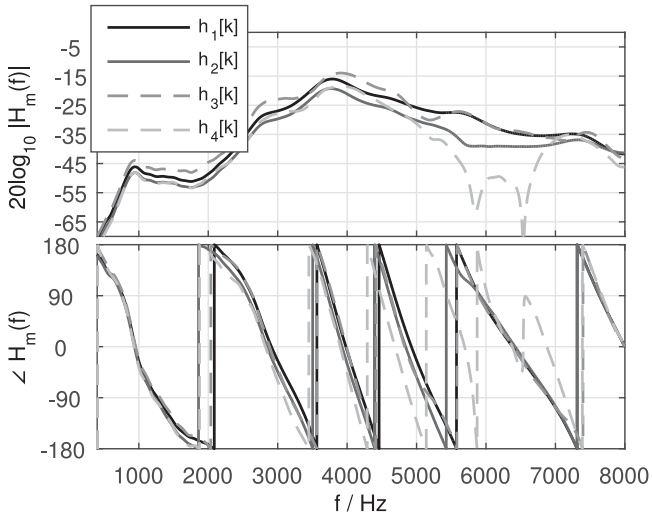


Fig. 2. Amplitude response (top) and phase response (bottom) of the first set of feedback paths for ear canals with diameter $d_1 = 7$ mm and length $l_1 = 15$ mm.

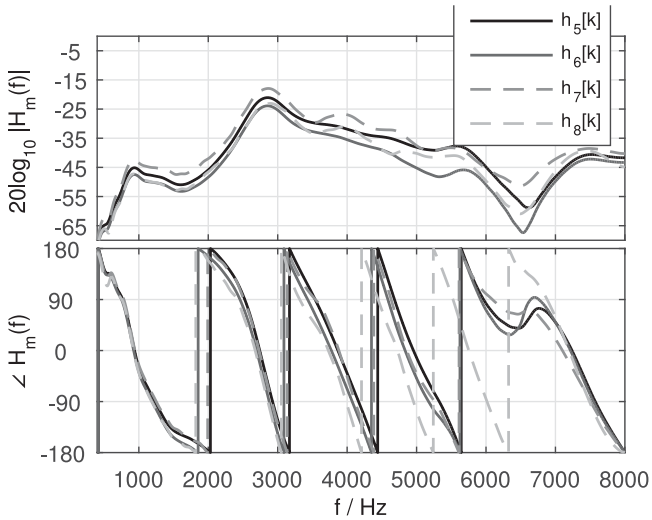


Fig. 3. Amplitude response (top) and phase response (bottom) of the second set of feedback paths for ear canals with diameter $d_2 = 8$ mm and length $l_2 = 20$ mm.

As performance measures we will use the average normalized misalignment and the ASG. The average normalized misalignment between the true, i.e., measured, IRs $\mathbf{h}_m$ and the estimated IRs $\hat{\mathbf{h}}_m$ is defined as

$$\xi = 10\log_{10}\frac{1}{|\mathcal{M}|}\sum_{m\in\mathcal{M}}\frac{\|\mathbf{h}_m-\hat{\mathbf{h}}_m\|_2}{\|\mathbf{h}_m\|_2}, \tag{51}$$

where $\mathcal{M}$ denotes the set of considered IRs and $|\mathcal{M}|$ its cardinality.

The ASG, i.e., the increase in gain of the hearing aid at which instability occurs due to an AFC algorithm, is used to quantify the allowable gain of the hearing aid. The average ASG of the set of acoustic feedback paths is defined as

$$\text{ASG} = 10\log_{10}\frac{1}{|\mathcal{M}|}\sum_{m\in\mathcal{M}}\frac{\max_\Omega|H_m(e^{j\Omega})|^2}{\max_\Omega|H_m(e^{j\Omega})-\hat{H}_m(e^{j\Omega})|^2}, \tag{52}$$

similarly to the definition of the MSG of [25], i.e.,

$$\text{MSG} = 10\log_{10}\frac{1}{|\mathcal{M}|}\sum_{m\in\mathcal{M}}\frac{1}{\max_\Omega|H_m(e^{j\Omega})-\hat{H}_m(e^{j\Omega})|^2}, \tag{53}$$

where $H_m(e^{j\Omega})$ and $\hat{H}_m(e^{j\Omega})$ denote the frequency response of the true, i.e., measured, ATF and the estimated ATF, respectively. Note that the closed-loop system is actually only unstable if also the phase at the frequency $\Omega$ corresponding to the minimum difference is a multiple of $2\pi$ [28] such that the definition in (53) is based on the worst-case assumption.

Similarly to the convergence criterion in [26], for all optimization procedures the sum of the normalized norm of the difference between successive common part coefficient vectors and successive variable part coefficient vectors, i.e.,

$$\frac{\|\mathbf{p}^c_{i-1}-\mathbf{p}^c_i\|_2}{\|\mathbf{p}^c_{i-1}\|_2}+\frac{\|\mathbf{b}^v_i-\mathbf{b}^v_{i-1}\|_2}{\|\mathbf{b}^v_{i-1}\|_2}<\varepsilon, \tag{54}$$

was used, where $\mathbf{p}^c_i=[\,(\mathbf{a}^c_i)^T\ (\mathbf{b}^c_i)^T\,]^T$ and $\varepsilon$ is a small positive constant which in this paper was chosen to be $\varepsilon=10^{-4}$. We used the following parameters for all simulations: For the QP-based approach $\delta=10^{-8}$, $Q=1024$ and for the SDP-based approach $\tau=10^{-8}$.

### B. Effect of Common Pole-Zero Initialization

Since all presented optimization procedures to estimate the common pole-zero filter aim to minimize a non-linear cost function, they may converge to a local minimum. Therefore, in general, a good initialization $\mathbf{a}^c_0$ and $\mathbf{b}^c_0$ (cf., Table I and II) is essential for all procedures. For all optimization procedures we tried different initializations over a wide range of parameters. For the equation-error based optimization procedure the best results were obtained when initializing the poles of the common pole-zero filter using the poles estimated from a common all-pole filter and $N^c_z+N^v_z$ variable zeros and initializing the zeros of the common pole-zero filter using a delta pulse. For the weighted equation-error based optimization procedure the best results were obtained, when initializing the poles of the common pole-zero filter using the poles estimated from the equation-error based optimization procedure and initializing the zeros of the common pole-zero filter using a delta pulse. Exemplary results are depicted in Fig. 4 for different initializations:

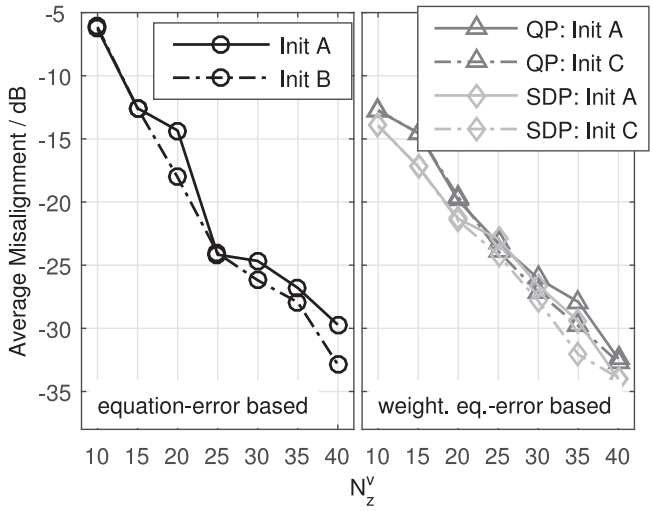


Fig. 4. Average normalized misalignment for different initializations of the common pole-zero filter using feedback paths $m=3,4$ ($N^c_z=6$, $N^c_z=4$).

(1) *Init A*: $\hat{\mathbf{b}}^c_0=[\,1\ 0\ \ldots\ 0\,]$ and $\hat{\mathbf{a}}^c_0=[\,0\ \ldots\ 0\,]$
(2) *Init B*: $\hat{\mathbf{b}}^c_0=[\,1\ 0\ \ldots\ 0\,]$ and $\hat{\mathbf{a}}^c_0$ was computed by minimizing (28) with $N^c_p$ common poles and $N^c_z+N^v_z$ variable zeros,
(3) *Init C*: $\hat{\mathbf{b}}^c_0=[\,1\ 0\ \ldots\ 0\,]$ and $\hat{\mathbf{a}}^c_0$ was obtained from the final results for the equation-error based optimization procedure using the same parameters of $N^c_p$, $N^c_z$ and $N^v_z$.

As can be observed from Fig. 4 for the equation-error based optimization procedure *Init B* leads to a lower misalignment compared to *Init A*, while for the weighted equation-error based optimization procedure *Init C* leads to a lower misalignment than *Init A*. The difference is observed to be as large as 4 dB. In the following hence *Init B* and *Init C* will be used for the equation-error based optimization procedure and the weighted equation-error based optimization procedure, respectively.

### C. Exemplary Comparison of Output-Error

The proposed weighted equation-error based optimization procedure is motivated by the observation that the equation-error based optimization procedure leads to poor estimation accuracy in the vicinity of large spectral peaks [16]. It is therefore expected that the weighted equation-error based optimization procedure leads to an increased accuracy in the vicinity of these spectral peaks. To demonstrate this, Fig. 5 shows the amplitude response of the first IR $h_1[k]$ and the amplitude responses of the corresponding output-errors for the equation-error based optimization procedure and the weighted equation-error based optimization procedures for both constraints. As expected the output-error for the weighted equation-error based optimization procedure is spread across the whole frequency range, whereas the output-error of the equation-error based optimization

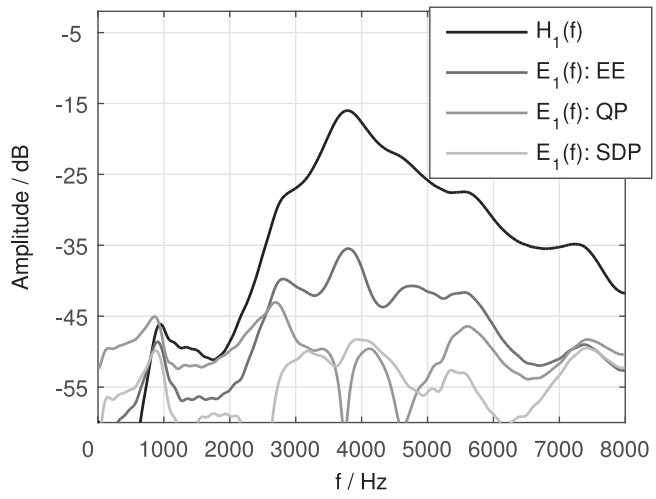


Fig. 5. Amplitude response of $\mathbf{h}_1$ and amplitude responses of the residual output-errors for all three optimization procedures ($N_p^c = 10$, $N_z^c = 0$, $N_z^v = 15$).

procedure more or less follows the spectral shape of $H_1(f)$. Hence, the largest peak in the output-error occurs in the frequency range of the largest peak of $H_1(f)$. In a hearing aid this would directly affect the MSG as defined in (53), which corresponds to the largest peak of the output-error signal. For the presented example the MSG is 35 dB for the equation-error based optimization procedure and 43 dB and 48 dB for the weighted equation-error based optimization procedure using the QP and SDP formulations, respectively. These results indicate that the weighted equation-error based optimization procedure successfully counteracts the weighting introduced in the equation-error based optimization procedure.

### D. Misalignment and ASG

To show the improved modeling accuracy of the weighted equation-error based optimization procedures for several choices of the parameters $N_p^c$, $N_z^c$, and $N_z^v$, simulations have been carried out for both acoustic scenarios (free field, telephone) separately. The impact of a change in the acoustic scenario on the validity of the common pole-zero filter is investigated in Section VI-E.

*1) Free Field:* Fig. 6 shows the average normalized misalignment for different choices of $N_p^c$ and $N_z^c$ as a function of $N_z^v$. The common and variable parts have been estimated for IRs measured in free field, i.e., $m = 1, 2$ (top row) and $m = 5, 6$ (bottom row). Note that for the right-most column ($N_p^c = 10$, $N_z^c = 0$) the results for the equation-error based optimization procedure correspond to the CAPZ model proposed in [13]. As can be observed the weighted equation-error based optimization procedures lead to a lower normalized average misalignment than the equation-error based optimization procedure. Furthermore, it can be observed that in general the SDP-based optimization procedure leads to a lower average normalized misalignment than the QP-based optimization procedure. Improvements of the SDP-based optimization procedure compared to the QP-based optimization procedure are in general consistent across different values of $N_z^v$, but tend to decrease for larger $N_z^v$. This can be intuitively explained by the larger amount of zeros being available to model the variable parts. Only for $N_p^c = 4$ and $N_z^c = 6$ for the second ear canal setup ($d_2 = 8$ mm, $l_2 = 20$ mm) the SDP-based optimization procedure is outperformed by the QP-based optimization procedure for $N_z^v = 20$, which can most likely be explained by the SDP-based optimization procedure converging to a poor local minimum. Comparison between the top and the bottom row shows that the assumption of a common pole-zero filter is valid for different ear canal geometries. Although the absolute improvements are slightly different, the same trends are visible.

Using the same parameter choices and IRs, Fig. 7 depicts the results for the average ASG. Similar as for the average normalized misalignment, the weighted equation-error based optimization procedures outperform the equation-error based optimization procedure. Furthermore, the proposed SDP-based optimization procedure using the Lyapunov constraint leads to the largest ASG of all optimization procedures. This is consistent with the results shown in Section VI-C.

For an increase in $N_p^c$ the weighted equation-error based optimization procedure using the SDP-based optimization in general outperforms the QP-based optimization procedure. This indicates that using the Lyapunov constraint in the SDP-based optimization procedure allows for an improved modeling accuracy and ASG compared to the positive realness frequency-domain constraint in the QP-based optimization procedure.

The use of the Lyapunov constraint is motivated by the fact that this constraint does not restrict the solution space as much as the positive realness constraint. To show that the positive realness constraint may be too restrictive, we consider the choice of $N_p^c = 10$, $N_z^c = 0$, $N_z^v = 10$, i.e., a common all-pole filter. For this parameter choice, the solution of the equation-error based optimization procedure using the ALS procedure in Table I converges to the globally optimal solution and is guaranteed to be stable, such that the stability constraints are actually not necessary. Fig. 8 depicts the pole locations for the equation-error based optimization procedure (without constraints) and when adding the stability constraints on the pole location using either the positive realness constraint (QP-based optimization procedure) or the Lyapunov constraint (SDP-based optimization procedure). As can be observed, the pole locations using the Lyapunov constraint coincide with the pole locations of the unconstrained equation-error optimization procedure, while the pole locations using the positive realness constraint are significantly different. This experimentally demonstrates the more restrictive effect of the positive realness constraint and the improved performance of the Lyapunov constraint.

*2) Telephone Receiver:* To investigate the performance for less similar feedback paths, Fig. 9 shows the average normalized misalignment for different choices of $N_p^c$ and $N_z^c$ as a function of $N_z^v$ using IRs measured in the presence of a telephone receiver, i.e., $m = 3, 4$ (top row) and $m = 7, 8$ (bottom row).

Similarly as for the free-field simulations in Fig. 6, both weighted equation-error based optimization procedures lead to a lower misalignment than the equation-error based optimization procedure. However, in general the improvements tend to

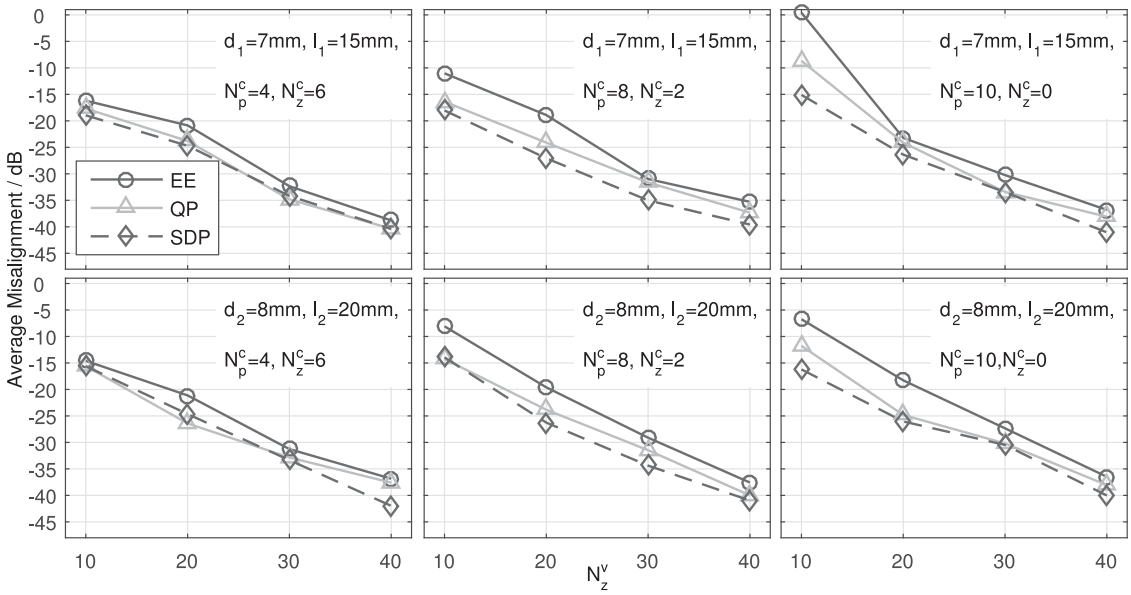


Fig. 6. Average normalized misalignment as a function of $N_z^c$ for different choices of $N_p^c$ and $N_z^c$ for several IRs measured in free field (cf., Table III).

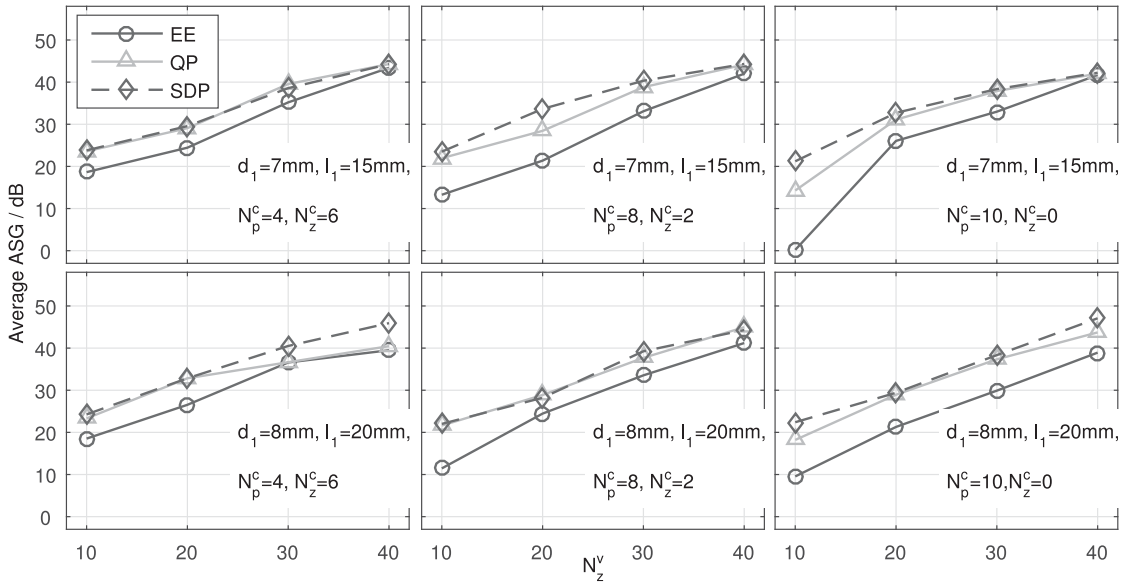


Fig. 7. Average ASG as a function of $N_z^c$ for different choices of $N_p^c$ and $N_z^c$ for several IRs measured in free field (cf., Table III).

be smaller for all considered combinations of $N_p^c$ and $N_z^c$. Similarly as for the free field simulations, the proposed SDP-based optimization procedure outperforms the QP-based optimization procedure, with the exception of $N_p^c = 4$ and $N_z^c = 6$ for the first ear canal setup ($d_1 = 7$ mm, $l_1 = 15$ mm), which can again most likely be explained by the SDP-based optimization procedure converging to a poor local minimum.

### *E. Robustness to Unknown Acoustic Scenarios*

In the previous sections the common pole-zero filter has been estimated using feedback paths measured in a single (static) acoustic scenario. While this allows to compare different estimation procedures, the estimated common pole-zero filter may not be robust to variations of the feedback path. Therefore, in

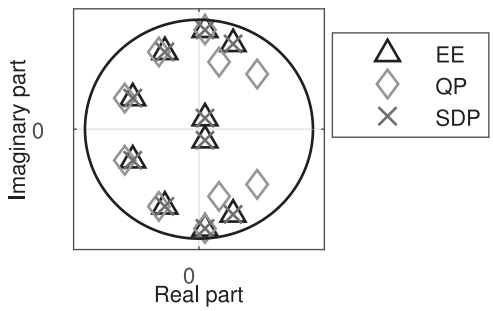


Fig. 8. Location of the poles for $N_p^c = 10$, $N_z^c = 0$, $N_z^v = 10$ using the equation-error based optimization procedure (without constraints) and when using constraints on the pole location used in the QP-based and SDP-based optimization procedures.

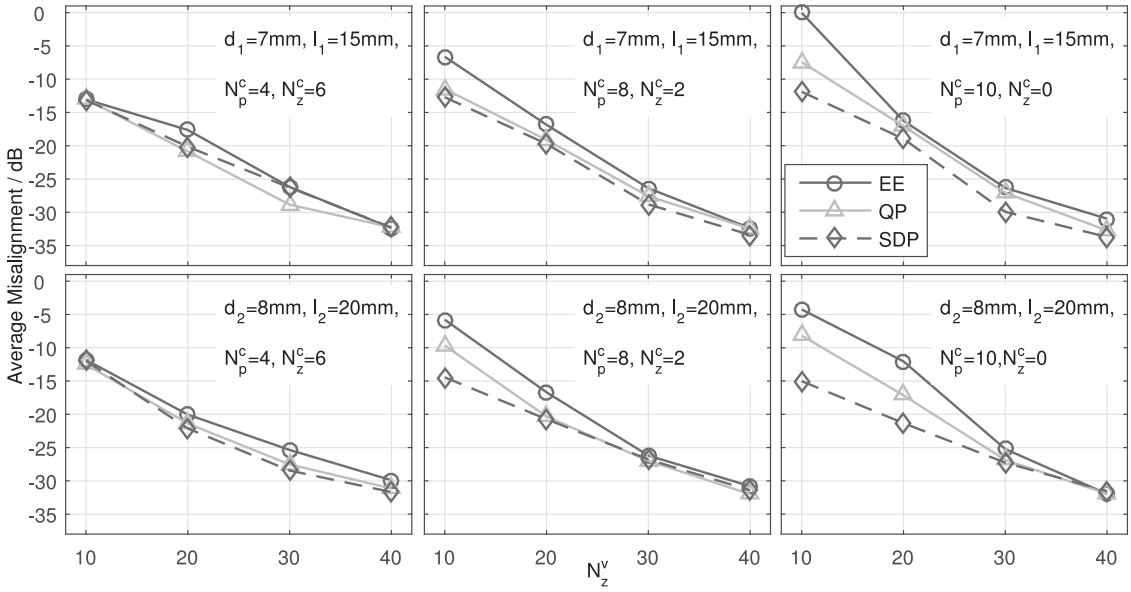


Fig. 9. Average normalized misalignment as a function of $N_z^v$ for different choices of $N_p^c$ and $N_z^c$ for several IRs measured in the presence of a telephone receiver (cf., Table III).

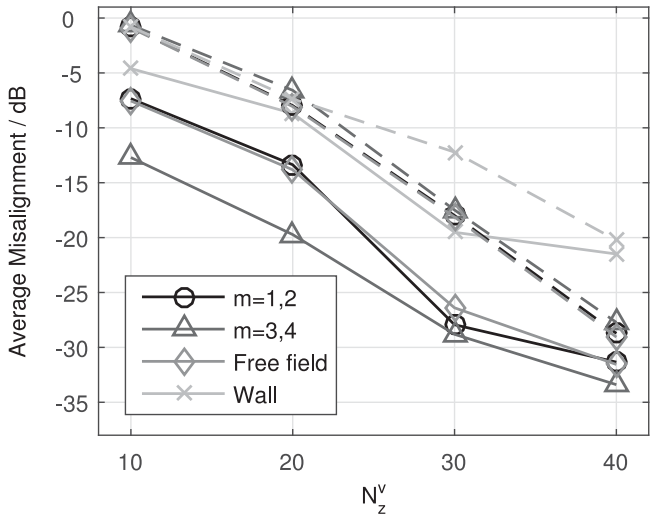


Fig. 10. Average normalized misalignment to investigate the robustness of the proposed optimization procedure as a function of $N_z^v$. The common pole-zero filter was estimated from IRs $m = 3, 4$ using $N_p^c = 8$ and $N_z^c = 2$. The variable parts were optimized assuming a fixed common pole-zero filter. Dashed lines indicate no common pole-zero filter, i.e., $N_p^c = N_z^c = 0$.

this sections simulations are performed where the common pole-zero filter is first estimated from IRs $m = 3, 4$ (in the presence of a telephone receiver) and then only the variable part coefficient vector $\mathbf{b}^v$ minimizing (32a) is estimated for a set of different IRs (assuming a fixed common pole-zero filter). This set of IRs included $m = 1, 2$ as well as four additional IRs, where two IRs were measured in free field after repositioning the hearing aid (*Free field*) and two IRs were measured with the dummy-head positioned close to a wall (*Wall*).

Fig. 10 depicts the average normalized misalignment when the common pole-zero filter is estimated using the proposed weighted equation-error based SDP-based optimization procedure using $N_p^c = 8$ and $N_z^c = 2$. As can be observed, in general the performance degrades for IRs that have not been included in the optimization of the common pole-zero filter. However, the average normalized misalignment of the proposed decomposition using the common pole-zero filter is better compared to modeling the IRs using only the variable part, i.e., $N_p^c = N_z^c = 0$, as indicated by the dashed lines.

To investigate the performance for the same number of coefficients required to model the complete feedback path, i.e., $N_z^v + N_p^c + N_z^c$, the same data are plotted in Fig. 11 as a function of the total number of coefficients. Performance in general can be considered similar for the proposed feedback path decomposition using the common pole-zero filter (solid lines) compared to not using this decomposition (dashed lines), however, for $N_z^v + N_p^c + N_z^c = 30$ this difference in performance is largest with about 5 dB. Nevertheless, these results show that, although an expected performance reduction for unknown feedback paths occurs, the proposed decomposition can lead to similar performance with fewer variable part parameters.

### F. Application to AFC in Hearing Aids

In this section we investigate the performance of the different optimization procedures to estimate the common part within an adaptive feedback canceller. We will consider a single-receiver-single-microphone AFC framework as depicted in Fig. 12. The incoming signal is denoted as $S(z)$, the microphone signal $Y(z)$ is processed by the hearing aid forward path $G(z)$ and played back by the loudspeaker. The loudspeaker and the microphone are coupled by the acoustic feedback path $H(z)$, yielding a closed-loop system. The (fixed) common part filter $\hat{H}^c(z)$ and the adaptive filter $\hat{H}^v(z)$ are used to subtract an estimate of the

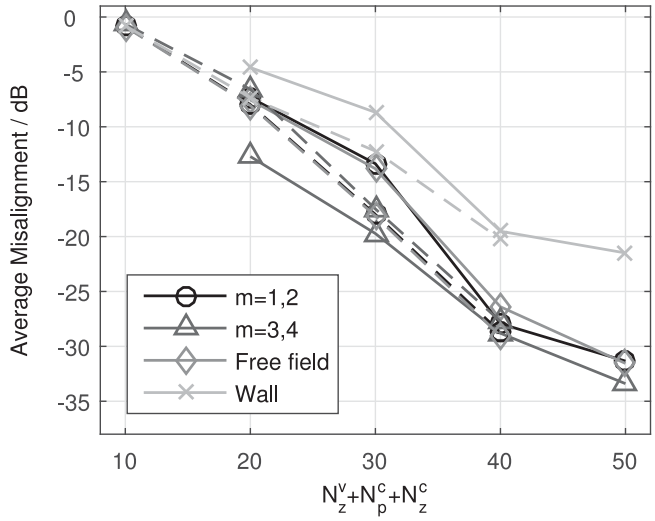


Fig. 11. Average normalized misalignment to investigate the robustness of the proposed optimization procedure as function of the total number of parameters required to model the feedback path, i.e., $N_z^v + N_p^c + N_z^c$. The common pole-zero filter was estimated from IRs $m = 3, 4$ using $N_p^c = 8$ and $N_z^c = 2$. The variable parts were optimized assuming a fixed common pole-zero filter. Dashed lines indicate the misalignment using no common pole-zero filter, i.e., $N_p^c = N_z^c = 0$.

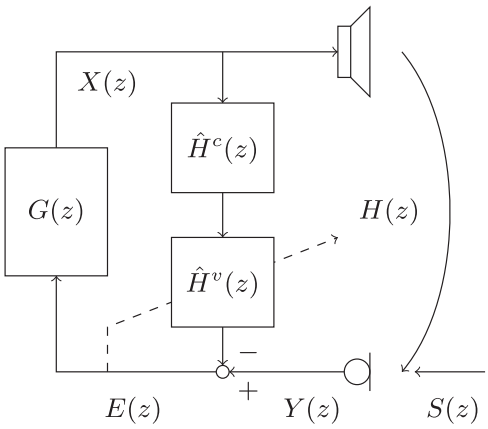


Fig. 12. Schematic of an AFC system using the common part decomposition.

feedback signal $\hat{H}^c(z)\hat{H}^v(z)X(z)$ from the microphone signal $Y(z)$, resulting in the error signal $E(z)$ which is used to the steer the adaptive filter $\hat{H}^v(z)$.

In our simulations the adaptive filter is updated using the normalized least mean squares (NLMS) algorithm in the time-domain. In order to reduce the bias of the estimated filter, the prediction-error method (PEM) [1], [29] is applied. As incoming signal we have used an 80s long speech signal comprising several male and female speakers as used in [30]. The hearing aid forward path was chosen as $G(z) = |G|z^{-d_G}$ with $|G| = 10^{(20/20)}$ and $d_G = 96$ corresponding to a delay of 6 ms at a sampling rate of $f_s = 16$ kHz. The prediction-error filter was estimated from the error signal $E(z)$ using the Burg-lattice algorithm [31], where the order of the prediction filter was set to $P = 9$. In all conditions the step-size of the NLMS algorithm was set to $\mu = 0.00025$.

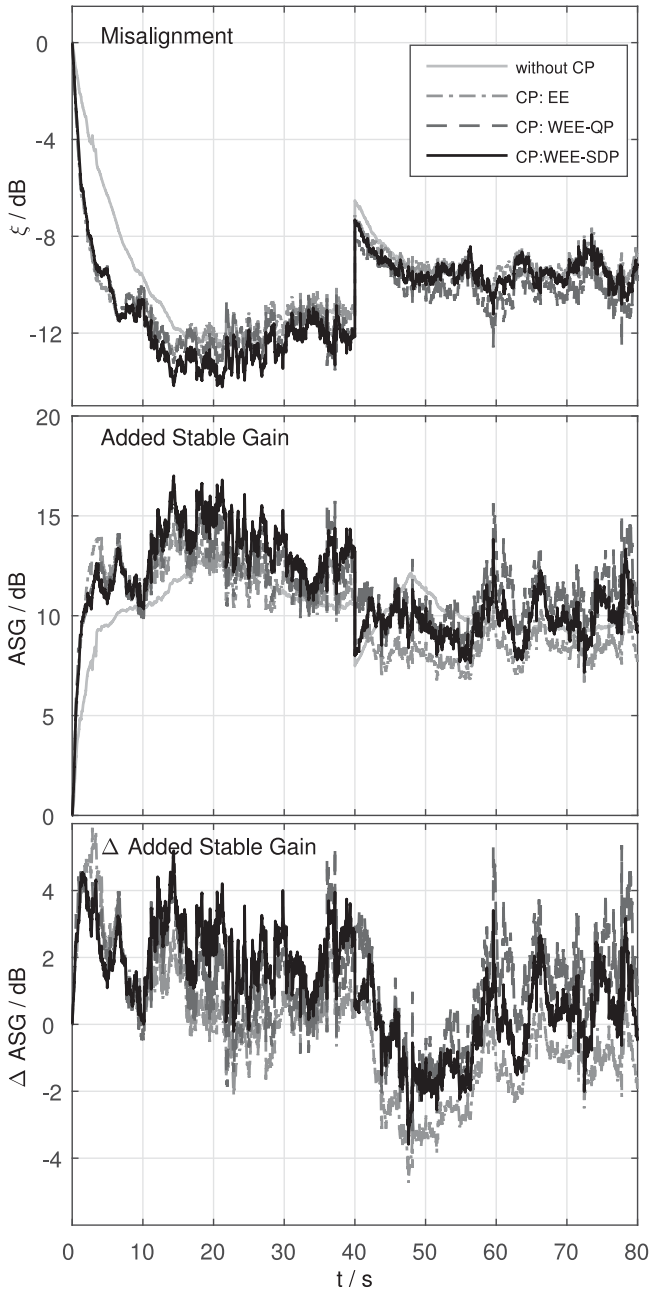


Fig. 13. Normalized misalignment (top) and ASG (mid) and ΔASG (bottom) as a function of time using an AFC algorithm without CP and an AFC algorithm using a common part obtained using the different optimization procedures. The ΔASG depicts the difference between the ASG using a common part and not using a common part.

Fig. 13 depicts the normalized misalignment and the ASG as well as the ΔASG as a function of time for the following two settings of the common and variable parts: 1) $N_p^c = 0$, $N_z^c = 0$, $N_z^v = 30$, i.e., without a common part, and 2) $N_p^c = 8$, $N_z^c = 2$, $N_z^v = 20$, i.e., using a common part estimated from the telephone receiver IRs $m = 3, 4$ for all three optimization procedures. The ΔASG was computed as the difference in ASG between using a common part, i.e., setting 2), and not using a common part, i.e., setting 1), for all optimization procedures. During the first 40 s the acoustic feedback path $m = 3$ was

used and during the remaining 40 s the acoustic feedback path $m = 1$ was used, which was not included in the optimization of the common part. In general, it can be observed that using a common part increases the convergence speed compared to not using a common part which has also been shown in [32]. During the first 40 s using the common part obtained from the weighted equation-error based optimization procedures outperforms using the common part obtained from the equation-error based optimization, where the common part obtained from the SDP-based optimization procedure yields the largest ASG and the lowest misalignment. This shows that similar results as in the previous sections can be achieved when the common part decomposition is applied in a state-of-the-art AFC algorithm. However, note that the differences in general appear smaller when adaptive algorithms are used to obtain an online estimate of the variable part. During the second half of the signal, the QP-based optimization procedure yields the highest ASG and lowest misalignment, indicating that in this case a better generalization to unknown feedback paths can be achieved by the common part obtained from the QP-based optimization procedure. While between 42 s–57 s the ASG when not using a common part is larger than the ASG when using a common part (approximately 1–2 dB), it should be noted that between 57 s–80 s using a common part outperforms not using a common part by approximately the same amount. Note that the performance can possibly be improved by increasing the set of acoustic feedback paths from which the common part is estimated, however, setting the requirements for such a set is beyond the scope of this work.

## VII. Conclusion

In this paper we proposed to estimate the common pole-zero filter of acoustic feedback paths in hearing aids using different least-squares optimization procedures. We provided a proof of the stability of the common pole-zero filter estimated using the equation-error based approach and incorporated two different stability constraints into the weighted equation-error based approach, leading to two different optimization problems. The first constraint is based on the positive realness of the frequency response of the common poles yielding a sufficient but not necessary condition for stability and leading to a QP-based optimization procedure. Furthermore, we propose a novel SDP-based optimization procedure which uses a Lyapunov constraint yielding sufficient and necessary conditions for the stability. Simulations using measured acoustic feedback paths from a two-microphone behind-the-ear hearing aid for different ear canal geometries showed that the weighted equation-error based optimization procedures enable to counteract the inherent weighting of the equation-error based optimization procedure. Moreover, it was experimentally shown that the proposed SDP-based optimization procedure of the weighted equation-error leads to the best modelling accuracy and the largest ASG. In addition, we demonstrated that, although a performance degradation occurs for unknown acoustic feedback paths, the proposed decomposition improves compared to using only the variable part. Simulations using a state-of-the-art AFC algorithm show that the convergence speed can be improved by using the common part decomposition and that the proposed weighted equation-error optimization procedures still yield the best modeling accuracy and ASG.

## Appendix A
## Stability of IRs Estimated Using Equation-Error Minimization

Proving the stability of the IRs estimated minimizing (14) for the special case $N_z^v = N_z^c = 0$, i.e., only considering common poles, has been done in [13]. For this special case, the closed-form solution in (29) reduces to

$$\mathbf{a}^c = -(\tilde{\mathbf{H}}^T \tilde{\mathbf{H}})^{-1} \tilde{\mathbf{H}}^T \tilde{\mathbf{h}}. \tag{55}$$

Since $\tilde{\mathbf{H}}^T \tilde{\mathbf{H}}$ is a symmetric positive definite matrix with Toeplitz structure, it can be shown that the all-pole filter $\frac{1}{A^c(z)}$ is stable [13], [33].

In the following we will show that this proof can be generalized to the case of arbitrary values of $N_z^v$ and $N_z^c$. For the problem at hand we only need to guarantee stability of the poles when minimizing (22b). Although a closed-form solution exists (cf., (26b)), minimizing (22b) can also be carried out using an alternating optimization procedure, i.e., minimizing at each iteration $l$

$$\begin{cases} J_{EE}^c \quad (\mathbf{b}_{i,l}^c) = \|\tilde{\mathbf{h}} + \tilde{\mathbf{H}}\mathbf{a}_{i,l-1}^c - \tilde{\mathbf{B}}_i^v \mathbf{b}_{i,l}^c\|_2^2, & \text{(56a)} \\ J_{EE}^c \quad (\mathbf{a}_{i,l}^c) = \|\tilde{\mathbf{h}} + \tilde{\mathbf{H}}\mathbf{a}_{i,l}^c - \tilde{\mathbf{B}}_i^v \mathbf{b}_{i,l}^c\|_2^2. & \text{(56b)} \end{cases}$$

The filter minimizing (56b) is equal to

$$\mathbf{a}_{i,l}^c = -(\tilde{\mathbf{H}}^T \tilde{\mathbf{H}})^{-1} \tilde{\mathbf{H}}^T (\tilde{\mathbf{h}} - \tilde{\mathbf{B}}_i^v \mathbf{b}_{i,l}^c), \tag{57}$$

where similar as in (55) $\tilde{\mathbf{H}}^T \tilde{\mathbf{H}}$ is symmetric, positive definite and of Toeplitz structure. Hence, at each iteration $l$ the all-pole filter $\frac{1}{A_{i,l}^c(z)}$ is stable. Since for $l \to \infty$ the filter $\mathbf{a}_{i,l}^c$ minimizing (56b) is equal to the closed-form solution $\mathbf{a}_i^c$ in (26b), also the filter $\mathbf{a}_i^c$ in (26b) is stable such that the common pole-zero filter minimizing (14) is stable.

## References


[1] A. Spriet, S. Doclo, M. Moonen, and J. Wouters, "Feedback control in hearing aids," in *Springer Handbook of Speech Processing*, J. Benesty, Ed., Berlin, Germany: Springer, 2008, pp. 979–999.

[2] T. van Waterschoot and M. Moonen, "Fifty years of acoustic feedback control: State of the art and future challenges," *Proc. IEEE*, vol. 99, no. 2, pp. 288–327, Feb. 2011.

[3] M. Guo, S. H. Jensen, and J. Jensen, "Novel acoustic feedback cancellation approaches in hearing aid applications using probe noise and probe noise enhancement," *IEEE Trans. Audio, Speech, Lang. Process.*, vol. 20, no. 9, pp. 2549–2563, Nov. 2012.

[4] C. R. C. Nakagawa, S. Nordholm, and W.-Y. Yan, "Feedback cancellation with probe shaping compensation," *IEEE Signal Process. Lett.*, vol. 21, no. 3, pp. 365–369, Mar. 2014.

[5] S. Haykin, *Adaptive Filter Theory*, 3rd ed. Englewood Cliffs, NJ, USA: Prentice-Hall, 1996.

[6] A. H. Sayed, *Fundamentals of Adaptive Filtering*. Hoboken, NJ, USA: Wiley, 2003.

[7] J. M. Kates, "Feedback cancellation apparatus and methods, U.S. Patent *6 072 884*, June 6, 2000.

[8] G. Ma, F. Gran, F. Jacobsen, and F. Agerkvist, "Extracting the invariant model from the feedback paths of digital hearing aids," *J. Acoust. Soc. Amer.*, vol. 130, no. 1, pp. 350–63, Jul. 2011.

[9] H. Schepker and S. Doclo, "Modeling the common part of acoustic feedback paths in hearing aids using a pole-zero model," in *Proc. Int. Conf. Acoust. Speech Signal Process.*, Florence, Italy, May 2014, pp. 3693–3697.
[10] H. Schepker and S. Doclo, "Estimation of the common part of acoustic feedback paths in hearing aids using iterative quadratic programming," in *Proc. Int. Workshop Acoust. Signal Enhancement*, Antibes, Juan Les Pins, France, Sep. 2014, pp. 46–50.
[11] C. J. Zarowski, X. Ma, and F. W. Fairman, "QR-factorization method for computing the greatest common divisor of polynomials with inexact coefficients," *IEEE Trans. Signal Process.*, vol. 48, no. 11, pp. 3042–3051, Nov. 2000.
[12] W. Qiu, Y. Hua, and K. Abed-Meraim, "A subspace method for the computation of the GCD of polynomials," *Automatica*, vol. 33, no. 4, pp. 741–743, Apr. 1997.
[13] Y. Haneda, S. Makino, and Y. Kaneda, "Common acoustical pole and zero modeling of room transfer functions," *IEEE Speech Audio Process.*, vol. 2, no. 2, pp. 320–328, Apr. 1994.
[14] P. Chin, R. M. Corless, and G. F. Corliss, "Optimization strategies for the approximate GCD problem," in *Proc. Int. Symp. Symbolic Algebraic Comp.*, Rostock, Germany, Aug. 1998, pp. 228–235.
[15] C. Mullis and R. Roberts, "The use of second-order information in the approximation of discreate-time linear systems," *IEEE Trans Acoust., Speech, Signal Process.*, vol. 24, no. 3, pp. 226–238, Jun. 1976.
[16] J. O. Smith III, *Introduction to Digital Filters: With Audio Applications*. W3K Publishing, vol. 2, 2007.
[17] K. Steiglitz and L. McBride, "A technique for the identification of linear systems," *IEEE Trans. Autom. Control*, vol. 10, no. 4, pp. 461–464, Oct. 1965.
[18] H. Fan and M. Nayeri, "On reduced order identification; revisiting on some system identification techniques for adaptive filtering," *IEEE Trans. Circuits Syst.*, vol. 37, no. 9, pp. 1144–1151, Sep. 1990.
[19] A. Chottera and G. Jullien, "A linear programming approach to recursive digital filter design with linear phase," *IEEE Trans. Circuits Syst.*, vol. 29, no. 3, pp. 139–149, Mar. 1982.
[20] W. S. Lu and A. Antoniou, "Design of digital filters and filter banks by optimization: A state of the art review," presented at the European. Signal Processing Conf., Tampere, Finland, Sep. 2000.
[21] W. S. Lu, S.-C. Pei, and C.-C. Tseng, "A weighted least-squares method for the design of stable 1-D and 2-D IIR digital filters," *IEEE Trans. Signal Process.*, vol. 46, no. 1, pp. 1–10, Jan. 1998.
[22] S. P. Boyd and L. Vandenberghe, *Convex Optimization*. Cambridge, U.K.: Cambridge Univ. Press, 2004.
[23] M. Grant and S. Boyd (2014, Mar.). CVX: MATLAB software for disciplined convex programming, version 2.1. [Online]. Available: http://cvxr.com/cvx
[24] M. Grant and S. Boyd, "Graph implementations for nonsmooth convex programs," in *Recent Advances in Learning and Control* ( Lecture Notes in Control and Information Sciences), V. Blondel, S. Boyd, and H. Kimura, Eds. New York, NY, USA: Springer, 2008, pp. 95–110.
[25] J. M. Kates, "Room reverberation effects in hearing aid feedback cancellation," *J. Acoust. Soc. Amer.*, vol. 109, no. 1, pp. 367–378, Jan. 2001.
[26] W. S. Lu, "Design of stable minimax IIR digital filters using semidefinite programming," in *Proc. IEEE Int. Symp. Circuits Syst.*, Geneva, Italy, May 2000, vol. 1, pp. 355–358.
[27] M. Hiipakka, M. Tikander, and M. Karjalainen, "Modeling the external ear acoustics for insert headphone usage," *J. Audio Eng. Soc.*, vol. 58, no. 4, pp. 269–281, Apr. 2010.
[28] H. Nyquist, "Regeneration theory," *Bell Syst. Tech. J.*, vol. 11, no. 1, pp. 126–147, 1932.
[29] A. Spriet, I. Proudler, M. Moonen, and J. Wouters, "Adaptive feedback cancellation in hearing aids with linear prediction of the desired signal," *IEEE Trans. Signal Process.*, vol. 53, no. 10, pp. 3749–3763, Oct. 2005.
[30] C. R. C. Nakagawa, S. Nordholm, and W.-Y. Yan, "Analysis of two microphone method for feedback cancellation," *IEEE Signal Process. Lett.*, vol. 22, no. 1, pp. 35–39, Jan. 2015.
[31] J. Makouhl, "Stable and efficient lattice methods for linear prediction," *IEEE Trans. Acoust., Speech, Signal Process.*, vol. AASP-25, no. 5, pp. 423–428, Oct. 1977.
[32] H. Schepker and S. Doclo, "A semidefinite programming approach to min-max estimation of the common part of acoustic feedback paths in hearing aids," *IEEE Trans. Audio, Speech, Lang. Process.*, vol. 24, no. 2, pp. 366–377, Feb. 2016.
[33] T. Ulrych and S. Treitel, "A new proof of the minimum phase property of the unit delay prediction error operator-revisited," *IEEE Trans. Signal Process.*, vol. 39, no. 1, pp. 252–254, Jan. 1991.

**Henning Schepker** (S'14) received the B.Eng. degree from the Jade University of Applied Sciences, Oldenburg, Germany, in 2011, and the M.Sc. degree (with distinction) from the University of Oldenburg, Oldenburg, Germany, in 2012, both in hearing technology and audiology. He is a currently working toward the Ph.D. degree at the Signal Processing Group, Department of Medical Physics and Acoustics, University of Oldenburg, Germany. His current research focuses on feedback cancellation for open-fitting hearing aids. His research interests include area of signal processing for hearing aids and speech and audio applications as well as speech perception.

**Simon Doclo** (S'95–M'03–SM'13) received the M.Sc. degree in electrical engineering and the Ph.D. degree in applied sciences from the Katholieke Universiteit Leuven, Leuven, Belgium, in 1997 and 2003, respectively. From 2003 to 2007, he was a Post-doctoral Fellow with the Research Foundation Flanders at the Department of Electrical Engineering, Katholieke Universiteit Leuven and the Adaptive Systems Laboratory, McMaster University, Hamilton, ON, Canada. From 2007 to 2009, he was a Principal Scientist with NXP Semiconductors at the Sound and Acoustics Group, Leuven, Belgium. Since 2009, he has been a Full Professor at the University of Oldenburg, Oldenburg, Germany, and a Scientific Advisor for the project group Hearing, Speech and Audio Technology of the Fraunhofer Institute for Digital Media Technology, Ilmenau, Germany. His research interests include signal processing for acoustical applications, more specifically microphone array processing, active noise control, acoustic sensor networks, and hearing aid processing. He received the Master Thesis Award of the Royal Flemish Society of Engineers in 1997 (with Erik De Clippel), the Best Student Paper Award at the International Workshop on Acoustic Echo and Noise Control in 2001, the EURASIP Signal Processing Best Paper Award in 2003 (with Marc Moonen), and the IEEE Signal Processing Society 2008 Best Paper Award (with J. Chen, J. Benesty, and A. Huang). From 2008 to 2013, he was a Member of the IEEE Signal Processing Society Technical Committee on Audio and Acoustic Signal Processing and the Technical Program Chair for the IEEE Workshop on Applications of Signal Processing to Audio and Acoustics in 2013. He has been a Guest Editor for several special issues (*IEEE Signal Processing Magazine, Elsevier Signal Processing*) and is an Associate Editor for IEEE/ACM TRANSACTIONS ON AUDIO, SPEECH, AND LANGUAGE PROCESSING and *EURASIP Journal on Advances in Signal Processing*.